

Tritium transport model at breeder unit level for HCLL breeding blanket

Original

Tritium transport model at breeder unit level for HCLL breeding blanket / Testoni, Raffaella; Candido, Luigi; Utili, Marco; Zucchetti, Massimo. - In: FUSION ENGINEERING AND DESIGN. - ISSN 0920-3796. - (2019).
[10.1016/j.fusengdes.2019.03.180]

Availability:

This version is available at: 11583/2730244 since: 2019-04-08T11:54:59Z

Publisher:

Elsevier Ltd

Published

DOI:10.1016/j.fusengdes.2019.03.180

Terms of use:

This article is made available under terms and conditions as specified in the corresponding bibliographic description in the repository

Publisher copyright

Elsevier postprint/Author's Accepted Manuscript

© 2019. This manuscript version is made available under the CC-BY-NC-ND 4.0 license
<http://creativecommons.org/licenses/by-nc-nd/4.0/>. The final authenticated version is available online at:
<http://dx.doi.org/10.1016/j.fusengdes.2019.03.180>

(Article begins on next page)

Tritium Transport Model at Breeder Unit Level for HCLL Breeding Blanket

Raffaella Testoni^a, Luigi Candido^a, Marco Utili^b, Massimo Zucchetti^a

^a *Dipartimento Energia, Politecnico di Torino, Corso Duca degli Abruzzi 24 – Torino, Italy*

^b *ENEA UTIS- C.R. Brasimone, Bacino del Brasimone, Camugnano, BO, Italy*

The Helium-Cooled Lithium Lead (HCLL) breeding blanket is one of the European blanket designs proposed for DEMO reactor. A tritium transport model is fundamental for the correct assessment of both design and safety, in order to guarantee tritium self-sufficiency and to characterize tritium concentrations, inventories and losses. The present 2D transport model takes into account a single breeder unit located in the outboard equatorial module of the HCLL breeding blanket, which is one of the most loaded modules in normal operating conditions. A multi-physics approach has been adopted considering several physics phenomena, providing for buoyancy effect, temperature fields, tritium generation rate and velocity profile of lead-lithium and coolant. The transport has been modelled considering advection-diffusion of tritium into the lead-lithium eutectic alloy, transfer of tritium from the liquid interface towards the steel (adsorption/desorption), diffusion of tritium inside the steel, transfer of tritium from the steel towards the coolant (recombination/desorption), advection-diffusion of diatomic tritium into the coolant. Tritium concentrations, inventories and losses have been derived under the above specified phenomena. In particular, the effect of buoyancy forces on the tritium transport has been implemented and compared with the condition without buoyancy.

Keywords: breeding blanket, DEMO, HCLL, tritium transport, buoyancy effect

1. Introduction

In fusion reactors, the prediction of tritium transport in lead-lithium liquid metal breeder blankets and the quantification of permeation rate from the lead-lithium into the helium coolant are fundamental [1]. Tritium transport and permeation allow to guarantee tritium self-sufficiency and to characterize tritium concentrations, inventories and losses. One of the goals is to control tritium permeation towards cooling system to an acceptable level [2] because if tritium would reach the environment, it could represent a potential radiological risk [3]. The development of a tritium transport model presents some issues due to the multi-physics of the system, multi-material domains, and complex blanket geometry. In literature it is possible to find some tritium transport models [2,4–11].

Four European breeding blankets designs have been proposed for DEMO reactor [12]. In this study, the Helium-Cooled Lithium-Lead (HCLL) has been considered. The objective of this work is to study the tritium transport at the minimal functional unit in the outboard equatorial module of HCLL, which is one of the most loaded modules in normal operating conditions. A multi-physics approach has been considered developing a 2D model, taking into account transport interface phenomena, tritium generation rate, velocity profile of lead-lithium and coolant, temperature field, and buoyancy effect. The calculations have been performed by means of Comsol Multiphysics 5.3a. In this paper, the results concerning tritium concentrations, inventories and losses will be shown. In particular, the influence of buoyancy effect on the tritium transport has been investigated.

2. Description of the model

2.1 Governing Equations and Solution Technique

A previous study [11] has been performed to investigate the tritium transport, taking into account the interface phenomena, tritium generation rate, velocity profile of lead-lithium and coolant, and temperature field. The scheme of the tritium phenomena is shown in that work [11]. In this study, the buoyancy effect has been introduced to analyze its impact on tritium transport.

The introduction of the buoyancy force in the Navier-Stokes equation of momentum could be very expensive in terms of computational time. The Boussinesq approximation is a way to treat buoyant flows without having to use the compressible formulation of the Navier-Stokes equations. The Boussinesq assumption can be applied to an incompressible fluid, as the lead-lithium is considered [13–16] due to the ratio between the density variation and variation lower than 1. It assumes that the density variation has no effect on the flow field, except the one which gives rise to a buoyancy force. The density is assigned to a reference value, ρ_0 [kg m⁻³], everywhere except in the volume force term, which is set to:

$$\vec{F} = (\rho_0 + \Delta\rho) \vec{g} \quad (1)$$

where \vec{g} is the gravity vector. Due to the fact that the density is constant everywhere except in the buoyancy term, the Navier-Stokes equations of mass conservation and momentum can be simplified as follows:

$$\nabla \cdot \vec{u} = 0 \quad (2)$$

$$\rho_0(\vec{u} \cdot \nabla \vec{u}) = -\nabla p + \mu \nabla^2 \vec{u} + (\rho_0 + \Delta \rho) \vec{g} \quad (3)$$

where \vec{u} [m s⁻¹] is the velocity field, p is the pressure [Pa], and μ [Pa s] is the dynamic viscosity.

In order to solve the velocity, pressure, temperature, buoyancy and concentration fields, an iterative procedure has been implemented. As a first step, Eqs (1-3) are simultaneously solved with the convective-conductive heat transfer equation:

$$\rho c_p \vec{u} \cdot \nabla T + \nabla \cdot (-k \nabla T) = \dot{Q} \quad (4)$$

where T [K] is the temperature, c_p [J kg⁻¹ K⁻¹] is the specific heat at constant pressure, k [W m⁻¹ K⁻¹] is the thermal conductivity and \dot{Q} [W m⁻³] is the volumetric heat generation rate. In the second step, the fluid motion in the coolant, which can be described by Reynolds Averaged Navier-Stokes (RANS) equations, has been solved. The buoyancy force acting on helium has not been considered, due to the low coolant density with respect to the density of the lead-lithium. The first two steps have been repeated until convergence of solution was reached. The steady state solution of temperature, pressure, velocity and buoyancy has been used as an input for the general tritium transport equation:

$$\frac{\partial c}{\partial t} + (\nabla \cdot \vec{u})c - \nabla \cdot (D \nabla c) = s \quad (5)$$

where c [mol m⁻³] is the tritium concentration in the i -th domain (lead-lithium, Eurofer, coolant), D [m² s⁻¹] is the diffusion coefficient of tritium and s [mol m⁻³ s⁻¹] is the molar tritium generation rate along the radial coordinate. For the steels, there is no tritium source and the process is governed by pure diffusion of tritium through the structures, whereas in the coolant tritium transport is governed by both advection and diffusion and no sources are present. A suitable set of boundary conditions have been adopted as reported in [11] to take into account continuity of the pressure at lead-lithium/steel interface, transfer of tritium from the liquid interface towards the steel, transfer of tritium from the steel towards the coolant, and advection-diffusion of diatomic tritium into the coolant, lead-lithium inlet temperature and coolant inlet temperature.

2.2 Inventories and losses

Starting from the estimated concentrations, tritium inventories have been evaluated:

$$I_{HCLL,i}(t) = M_T \cdot L_{tor} \cdot \iint c_i(\vec{x}, t) \cdot dA_i \quad (6)$$

where $I_{HCLL,i}$ [g] is the tritium inventory for the HCLL BU in the i -th domain (Pb-15.7Li, Eurofer and helium), M_T [g mol⁻¹] is the atomic/molecular weight of tritium, L_{tor} [m] is the length of HCLL BU in toroidal direction, c_i [mol m⁻³] is the concentration. The integral has been evaluated on the radial-poloidal area of the i -th domain.

On the other hand, tritium losses have been defined as the ratio of the tritium permeated through the Eurofer

CPs and hSPs to the total tritium generated inside the lead-lithium eutectic:

$$\Phi_{HCLL}(t) = 100 \cdot \frac{\int J_{perm}(\vec{x}, t) \cdot dl}{\iint s(\vec{x}, t) \cdot dA_{LM}} \quad (7)$$

where Φ_{HCLL} [%] is the tritium losses in HCLL BU and J_{perm} [mol m⁻² s⁻¹] is the total flux which permeates from the Pb-15.7Li domain into the Eurofer domain.

2.3 Tritium balance

Tritium balance in the lead-lithium must be satisfied at each time step of the computation: for this purpose, a mass balance equation has been imposed. Since the inlet flux is zero, generation must be equal to the accumulation of tritium plus the flux which exits the lead-lithium domain, i.e. the flux permeated into the steel plus the flux exiting from the lead-lithium eutectic outlet. The tritium balance equation can be written as follows:

$$\begin{aligned} & L_{tor} \cdot \left[\iint s(\vec{x}, t) \cdot dA \right] \\ & \quad \text{Generation} \\ & = L_{tor} \left[\sum_{i=1}^{n_p} \int J_{perm,i}(\vec{x}, t) \cdot dl_i + \int J_{out}(\vec{x}, t) \cdot dl \right] \\ & \quad \text{Outlet} \\ & + \left[\frac{\partial}{\partial t} \iint c_1(\vec{x}, t) \cdot dA \right] \\ & \quad \text{Accumulation} \end{aligned} \quad (8)$$

where L_{tor} [m] is the toroidal length of the BU, s [mol m⁻³ s⁻¹] is the tritium generation rate, A [m²] is the radial-poloidal surface area of the lead-lithium eutectic domain, n_p is the number of permeations surfaces, indicated with subscript i , J_{perm} [mol m⁻² s⁻¹] is the tritium permeation flux entering in the steel [2], J_{out} [mol m⁻² s⁻¹] is the tritium flux exiting from the lead-lithium outlet, c_1 [mol m⁻³] is the tritium concentration in the liquid metal.

3. Input data

The optimised-conservative design is considered [17], for which the HCLL breeder unit geometry is characterized by 3 manifold, two horizontal stiffening plates (hSPs), two vertical stiffening plates (vSPs) and two cooling plates (CPs). For this study, the tritium transport has been developed in radial-poloidal direction (Fig.1).

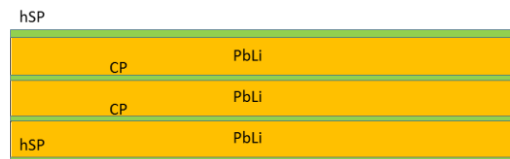


Fig. 1 Optimised-conservative design of the breeder unit [11].

Starting from work [11], the same assumption on the thermo-fluid-dynamic analysis has been made. In Table 1, the main input data are reported.

Table 1. Main input data [11].

Parameter	Value	Description
$T_{in,LM}$	331 [°C]	Pb-15.7Li inlet temperature
p_{LM}	5 [bar]	Pb-15.7Li inlet pressure
v_{LM}	1 [mm s ⁻¹]	Pb-15.7Li inlet velocity
Φ_{sup}	0.5 [MW m ⁻²]	Thermal heat flux on the first wall
$T_{He,CP}$	350 [°C]	He inlet temp. into CPs
$T_{He,hSP}$	300 [°C]	He inlet temp. into hSPs
$v_{He,CP}$	70 [m s ⁻¹]	He inlet velocity into CPs
$v_{He,hSP}$	50 [m s ⁻¹]	He inlet velocity into hSPs
p_{He}	80 [bar]	Helium inlet pressure

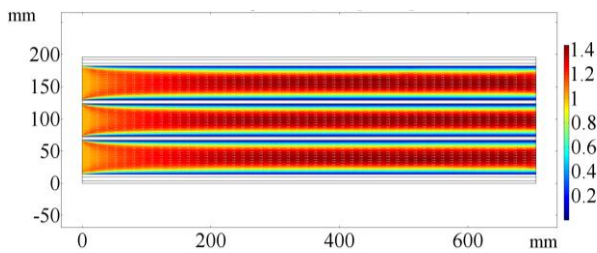
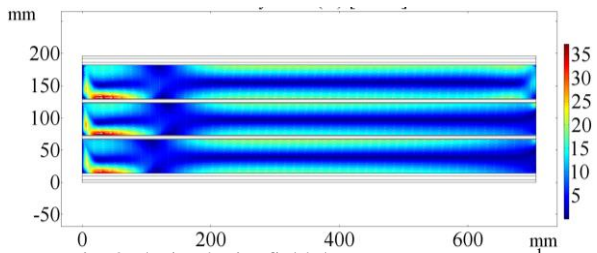
4. Results

In this section, the main results are shown underling the effect of buoyancy on velocity fields, temperature fields, and in particular on the tritium transport.

4.1 Thermo-fluid-dynamics calculation

Firstly, the effect of buoyancy forces has been investigated analyzing the impact on the velocity field of lead-lithium. As far as the velocity field without buoyancy forces is concerned, it is shown in Fig.2 and corresponds to an inlet velocity of 1 [mm s⁻¹]. The full developed profile lead to a maximum lead-lithium outlet velocity in the centre of the fluid equal to 3.5 [mm s⁻¹]. The introduction of buoyancy forces strongly modifies the velocity field (Fig.3). In particular, the high lead-lithium density value influences the volume forces (eq.3), with the creation of re-circulation patterns. The maximum velocity is reached in the flow pattern at the left, with a maximum value of 36 [mm/s].

The temperature field is similar to that one of velocity. It is important to underline that the buoyancies tend to “smooth” the temperature distribution, leading to a decrease in the maximum temperature in the PbLi of about 20%. Without buoyancy, the maximum temperature in PbLi is 531 [°C], instead the case with buoyancy reaches 429 [°C].

Fig. 2 PbLi velocity field, no buoyancy case [mm s⁻¹].Fig. 3 PbLi velocity field, buoyancy case [mm s⁻¹].

4.1 Tritium transport

The transport of tritium has been studied under no pulsed operative conditions, i.e. with a tritium generation rate as a decreasing exponential function in the radial direction but constant in time. Tritium concentrations inside the Pb-15.7Li, Eurofer and Helium are reported in Figures 4, 5, and 6, respectively, comparing the case without (NB) and with buoyancy (B). The tritium concentration in the lead-lithium tends to be increased under the action of the buoyancy force; this is due to the fact that the temperature field is modified and the average temperature is reduced: then, the diffusion coefficient, Sieverts’ constant, recombination and dissociation constant tend to decrease when the local temperature decreases. Consequently, the concentration in Eurofer increases since the permeation flux is higher, so as at the interface Eurofer/helium the permeation flux in the buoyancy case is increased, since more tritium permeates into the coolant. As reported in Table 2, it can be observed that there is a delay in the time to reach the asymptotic condition in the case with buoyancy effect. The long response time of the case without buoyancy, where diffusion is dominant respect to advection, is reduced due to the presence of vortexes, which locally increase the the velocity and then the advection contribution. This cause a higher retention in the PbLi domain. The maximum variation in terms of equilibrium concentration is found in Eurofer, with a difference of 30.0%. In Table 3, the equilibrium inventories and losses are evaluated. It must be observed that the value of inventories refers to the equilibrium condition. The differences in the total inventory is due to the numerical error (about 10%) arising from the numerical evaluation of concentrations and inventories.

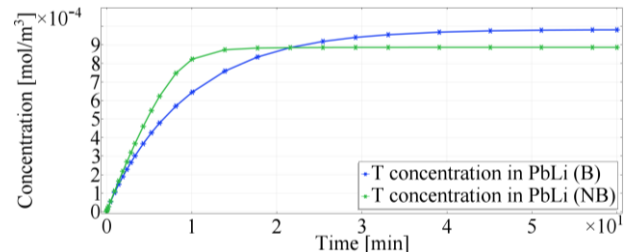


Fig. 4 Average T concentration in Pb-15.7Li.

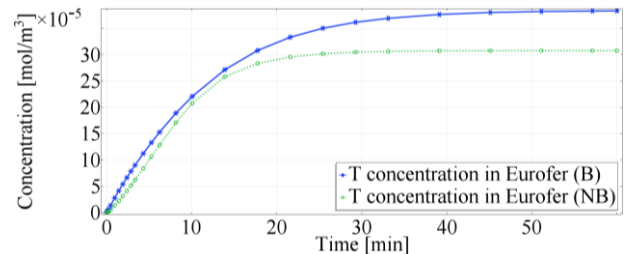


Fig. 5 Average T concentration in Eurofer.

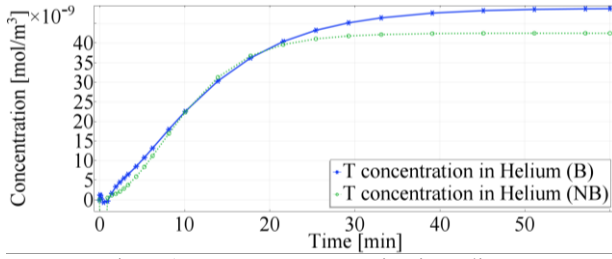


Fig. 6 Average T_2 concentration in Helium.

Table 2. Equilibrium concentrations in HCLL breeder unit.

	$c_{eq,B}$ [mol m ⁻³]	$c_{eq,NB}$ [mol m ⁻³]	t_B^* [min]	t_{NB}^* [min]
T in Pb-15.7Li	$9.82 \cdot 10^{-4}$	$8.87 \cdot 10^{-4}$	42	16
T in Eurofer	$3.84 \cdot 10^{-4}$	$3.08 \cdot 10^{-4}$	44	29
T_2 in Helium	$4.88 \cdot 10^{-8}$	$4.25 \cdot 10^{-8}$	45	28

Table 3. Equilibrium inventories and losses in HCLL BU.

	Inventories	
	With buoyancy	Without buoyancy
T in Pb-15.7Li [μg]	47.32	42.75
T in Eurofer [μg]	2.39	1.92
T_2 in Helium [μg]	$6.38 \cdot 10^{-4}$	$5.55 \cdot 10^{-4}$
Total [μg]	49.71	44.67
Losses		
Losses to CPs [%]	12.0	7.1
Permeation to hSPs [%]	1.3	1.2
Total [%]	13.3	8.3

In Figures 7 and 8, the mass balance obtained is reported as a function of the physical time, i.e. the time needed to reach the asymptotic condition. Tritium molar rate exiting the breeder unit decreases when considering the buoyancy effect, whereas an increase in the permeation flux towards the CPs and the hSPs is shown. This means that a higher concentration in the Eurofer material is expected, and a lower concentration in the eutectic alloy is foreseen. Moreover, since a higher concentration in the Eurofer is found, the tritium flux exiting from this domain and entering in the helium domain is expected to increase. The average error in the mass balance is 9% for the buoyancy case and 0.2% in the no buoyancy case. The increase of the error can be due to the numerical errors related to the increased non-linearity in the buoyancy partial differential equations.

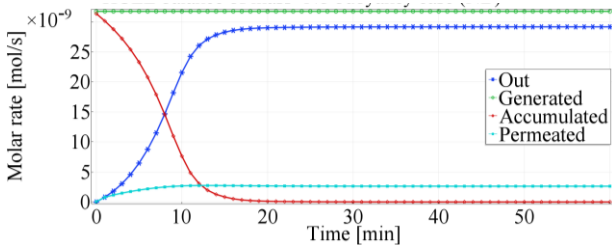


Fig. 7 Representation of the mass balance in no buoyancy case.

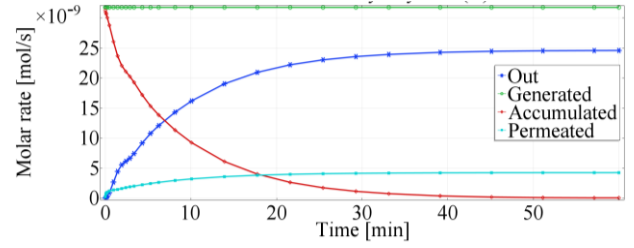


Fig. 8 Representation of the mass balance in buoyancy case.

5. Conclusions

A tritium transport study has been performed for HCLL at breeder unit level with a multi-physics approach, including interface phenomena, tritium generation rate profile, thermal fields, velocity field of both lead-lithium and coolant. Starting from a reference case [11], buoyancy forces have been implemented.

Concerning the velocity field, it is strongly modified due to the action of buoyancy force, with a formation of vortices which locally accelerates the flow in proximity of the lead-lithium inlet and outlet.

A second important effect of buoyancy is that inhomogeneities in the temperature field are smoothed out, causing the maximum temperature to decrease.

From the tritium concentration viewpoint, it appeared that the buoyancy force tends to slightly increase the tritium concentration of the liquid metal and increases tritium losses. However, the major effect of the buoyancy is to increase the time needed to reach the equilibrium condition.

Future works will regard the integration of magneto-hydro-dynamics in order to investigate the direct effect on the velocity field and as consequences the impact on the tritium concentrations, inventories and losses.

References

- [1] S. Malang, et al., An example pathway to a fusion power plant system based on lead-lithium breeder: comparison of the dual-coolant lead-lithium (DCLL) blanket with the helium-cooled lead-lithium (HCLL) concept as initial step, *Fusion Engineering and Design* 84 (2009) 2145–2157.
- [2] L. Candido, et al., Tritium transport in HCLL and WCLL DEMO blankets, *Fusion Engineering and Design* 109–111 (2016) 248–254.
- [3] U. Fischer, et al., Neutronics requirements for a DEMO fusion power plant, *Fusion Engineering and Design* 98–99 (2015) 2134–2137.
- [4] H. Zhang, et al., Quantification of dominating factors in tritium permeation in PbLi blankets, *Fusion Science and Technology* 68 (2015) 362–367.
- [5] P. Zhao, et al., Tritium transport analysis for CFETR WCSB blanket, *Fusion Engineering and Design* 114 (2017) 26–32.
- [6] L. Pan, et al., Tritium transport analysis of HCPB blanket for CFETR, *Fusion Engineering and Design* 113 (2016) 82–86.
- [7] F. Franza, et al., Tritium transport analysis in HCPB DEMO blanket with the FUS-TPC code, *Fusion Engineering and Design* 88 (2013) 2444–2447.

- [8] L. Batet, et.al, Mathematical models for tritium permeation analysis in liquid metal flows with helium bubbles, *Fusion Engineering and Design* 89 (2014) 1158–1162.
- [9] F. Ugorri, et al., Preliminary system modeling for the EUROfusion water cooled lithium lead blanket, *Fusion Science and Technology* 71 (2017) 444–449.
- [10] E. Carella, et al., Tritium behavior in HCPB breeder blanket unit: modeling and experiments, *Fusion Science and Technology* 71 (3) (2017) 357–362.
- [11] L. Candido, et al., Tritium transport model at the minimal functional unit level for HCLL and WCLL breeding blankets of DEMO, *Fusion Engineering and Design* (2018) (in press) <https://doi.org/10.1016/j.fusengdes.2018.05.002>
- [12] D. Maisonnier, et al., DEMO and fusion power plant conceptual studies in Europe, *Fusion Engineering and Design* 81 (8–14) (2006) 1123–1130.
- [13] S. Smolentsev, et al. Current approaches to modeling mhd flows in the dual coolant lead lithium blanket. *Magnetohydrodynamics* 42 (2-3) (2006) 225–236.
- [14] E. Mas de les Valls, et al. Influence of thermal performance on design parameters of a He/LiPb dual coolant DEMO concept blanket design, *Fusion Engineering and Design*, 87 (7–8) (2012) 969-973.
- [15] L. Bühler and C. Mistrangelo, MHD flow and heat transfer in model geometries for WCLL blankets, *Fusion Engineering and Design*, 124 (2017) 919-923.
- [16] Zhi-Hong Liu, et al. Effects of magnetohydrodynamic mixed convection on fluid flow and structural stresses in the DCLL blanket, *International Journal of Heat and Mass Transfer*, 135 (2019) 847-859
- [17] J. Aubert et al., HCLL Design Report 2016, Final Report on Deliverable, No. BB-2.2.1-T003-D001, 2017.